International Journal for Housing Science and Its Applications
Publish August 4, 2025. Volume 46, Issue 3 Pages 2768-2784

https://doi.org/10.70517/ijhsa463233

Personalized Design Applications and Innovations in Ceramic Art Creation Using 3D Printing

Zheng Yuan[1,*]
[1] Zhengzhou Academy of Fine Arts, Zhengzhou, Henan, 450000, China
Corresponding authors: (e-mail: 13683835853@163.com).

Abstract The emergence of 3D printing technology has brought about a revolutionary change in the creation and design of ceramic artwork, which is not only able to quickly and accurately produce complex ceramic structures, but also able to achieve personalized customization and creative design, which has injected a new vitality into ceramic art. In this paper, after analyzing the application status of 3D printing technology in personalized ceramic artwork, we explored the method of generating the image of ceramic artwork based on genetic algorithm, after comparing the traditional and multi-objective optimization two kinds of 3D printing task scheduling methods, we established a 3D printing multi-objective optimization task scheduling problem model, combined with the improvement of particle swarm algorithm for solving the problem, and got the closest point to the ideal point as the optimal solution as: θ_1 =180°, h=0.201mm, ΔV =336.22mm3, T=342. In the analysis of ceramic artwork modeling based on perceptual imagery, it is found that the perceptual vocabulary corresponding to Sample 2 and Sample 3 is more inclined to the rounded, simple, and practical among the four influencing variables of the structural factors.

Index Terms genetic algorithm, improved particle swarm algorithm, 3D printing technology, ceramic artwork

I. Introduction

For a long time, the design and development of ceramic handicrafts have been constrained by factors such as tools, materials and processes [1], [2]. With the progress of science and technology and aesthetic changes, ceramic tools and materials and molding processes have been continuously developed and improved for thousands of years, and consequently the shape, appearance, style and personalization of ceramic handicrafts have become more and more rich [3]-[6]. 3D printing technology is a product of the current digital age, the use of this technology in the development of ceramic creative design, not only from a technical point of view to improve the efficiency of the development, but also for the design of ceramic handicrafts to bring new ideas and new inspiration [7]-[10].

3D printing technology is based on digital models, the use of powdered metal or plastic and other bondable materials, through the way of layer-by-layer printing to construct the object of the technology, which has the advantages of simple operation, fast molding speed, high accuracy, etc. [11]-[14]. In the design phase of 3D modeling, one of the most computer resource-saving way is to use as few points and lines and surfaces combined and arranged to form as rich as possible three-dimensional shape, this design idea is called the 3D model of the industry of low-mode “topology” [15]-[18]. This topological structural features applied to 3D ceramic crafts modeling design, so that designers can get rid of the traditional handmade craft modeling limitations, the use of digital modeling of the form language for the design of the composition, more emphasis on the craft modeling of the geometric sense of form of the combination of points, lines and surfaces, rich in the modernist atmosphere [19]-[22]. Combined with the fine layer height printing, the production of exquisite modern abstract geometric style crafts, to the market and consumers to provide more modern aesthetic experience, to avoid the aesthetic homogenization and lack of personalization of traditional ceramic handicraft products on the market, to provide a more rich in the characteristics of the times ceramic craft products [23]-[26].

This paper firstly discusses the application of 3D printing technology in the design and creation of ceramic artwork. Subsequently, it proposes the image generation method of ceramic artwork based on genetic algorithm, and then compares the traditional and multi-objective optimization two 3D printing task scheduling methods, and at the same time, adopts the n-paradigm weighting method to allocate weights for different optimization objectives to form a combination of optimization objectives, and establishes the 3D printing multi-objective optimization task scheduling problem model. After that, based on the improved particle swarm algorithm, the average cost per unit volume is used as the adaptation degree, the scheduling sequence is used as the position information of the particles, the solution of the problem is represented by the decimal sequential two-dimensional encoding, and the dynamic inertia factor with linear decreasing weights is applied to the updating strategy to adjust the global and local searching

ability, which in turn obtains the optimal value of the objective function and the corresponding solution set. In the experimental part, the performance of the improved genetic algorithm proposed in this paper is tested, and at the same time, an example ceramic artwork model is selected to verify the feasibility of this paper's method and to evaluate the perceptual intention.

II. 3D printing technology in ceramic art creation in the application of practice

(1) Innovation at the design stage

In traditional ceramic art creation, designers usually need to rely on hand-drawing or sculpture to build the shape and structure of the work. However, this approach is often limited by the level of technology and material properties, making it difficult to realize complex and detailed designs. The introduction of 3D printing technology has solved this problem. Artists through the 3D modeling software to freely build complex shapes and structures, to achieve the effect of the traditional process is difficult to achieve. 3D software also provides a rich library of materials and textures, so that artists can more realistically simulate the texture and appearance of ceramics. Using virtual simulation technology, the artist can also preview and adjust the effect of the work in the design process, greatly improving the efficiency and quality of the design.

(2) Optimization of the production stage

In the production process of ceramic works, the traditional method requires a number of trial production and modification to achieve satisfactory results. This is not only time-consuming and labor-intensive, but also costly. 3D printing technology, on the other hand, can realize the rapid conversion from design to production and greatly shorten the production cycle. Through 3D printers, artists can directly print out the designed model as the prototype of the ceramic work. 3D printing is not only fast and accurate, but also can avoid the error and waste of manual production. At the same time, 3D printing technology can also achieve the optimal use of ceramic materials, reduce the generation of waste and lower production costs. In addition, 3D printing technology can also be applied to the surface decoration and texture treatment of ceramics. By printing out films or coatings with specific textures and patterns, artists can add more artistic effects and personalized elements to ceramic works.

(3) The realization of personalized customization

With the diversification of consumer demand, personalized customization has become an important trend in the ceramic art market. And 3D printing technology provides strong support for the realization of personalized customization. Artists can use 3D scanning technology to obtain the consumer's facial or physical characteristics and specific things characteristic data, and then according to these data to customize a unique ceramic artwork. Such customized works not only meet the consumer's personalized needs, but also has a high commemorative significance and collection value. In addition, the artist can also through online platforms or social media and other channels, interaction and communication with consumers, to understand their preferences and needs, so as to design ceramic artwork more in line with market demand. This interactive way of creation can not only improve the creativity and market competitiveness of the works, but also enhance the contact and interaction between artists and consumers.

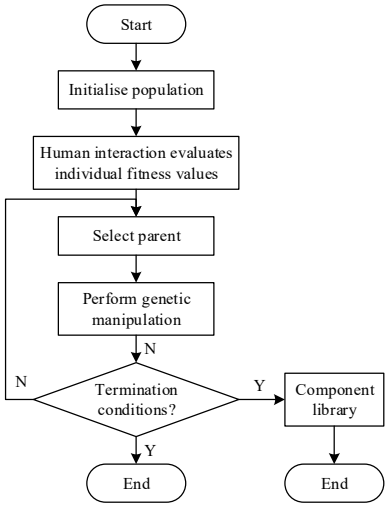

Figure 1: Ceramic construction innovation design process

III. Research on multi-task scheduling strategy for 3D printing based on improved genetic algorithm

III. A. Genetic Algorithm Based Image Generation Method for Ceramic Artwork

III. A. 1) Design process of ceramic model based on genetic algorithm

If a shape wants to evolve, the first step is population generation, which is based on the criteria of the component shape, and then the resulting population is evolved in detail. The evolutionary process needs to be precise, especially between each individual, to rationalize the calculation of whether the population is adapted to them or not. After selecting the parent individual, genetic operations are performed to verify whether the termination conditions are met [27]. The ceramic construction innovation design process is shown in Figure 1.

III. A. 2) Adaptation function

Among genetic algorithms, individual performance is an important description, and the main index of this performance is the fitness, which mainly determines the selection criteria of individuals. In this paper, the calculation method of fitness will be accomplished according to two scaling criteria. The first scale criterion is the optimal structure line ratio, which can be set by both seed structure line ratio and manually input structure line ratio. The second scaling criterion is the current individual structural line ratio.

Taking a certain construction as an example, assuming that it has n structural lines and two of the ratio criteria have been specified, Equation (1) can be derived, i.e., calculating the fitness of an individual. Where $Best_i$ is the ratio, which represents the ratio of the first ratio criterion, i.e., the radius of the i th structural line to the l th structural line. And $Current_i$ represents the ratio between the two structural lines (i and l).

$$fitness_i = \frac{1}{\sum_{i=1}^{n} \frac{\left|Best_i - Current_i\right|}{Best_i}} \tag{1}$$

The $fitness_i$ represents the fitness function, the larger the value of which proves that the individual has a higher fitness value, i.e., it is more likely to adapt to unfamiliar environments, and thus more likely to be bred.

III. A. 3) Variant operations

If a new individual does not reach a mature state of suppression it is called a mutation operation, which serves to maintain population diversity and is used to search for areas that are difficult to find. Thus, in the same population batch, the superiority or inferiority of each individual determines their mutation probability. If an individual has more disadvantages, the higher its probability of generating variation. Conversely, an individual that is of higher quality will have very little probability of developing mutations. In this regard, in order to prevent too much precocity from occurring, the degree of precocity was analyzed in detail and the following method was devised to be able to adapt to the probability of variation so that the population can remain in a state of diversity.

$$P_m = \frac{P_{m\max} - P_{m\min}}{2\left(f - f_{avg}\right)} P_{m\max} \quad f \le f_{avg} \tag{2}$$

$$P_m = \frac{P_{m\min}}{1 + \exp\left\{\Delta\left[\frac{2(f - f_{avg})}{f_{\max} - f_{\min}}\right]\right\}} \quad f > f_{avg} \tag{3}$$

In the above equation, $P_{m\min}$, $P_{m\min}$ represented by are constants, the value of the adaptation of the variant individuals is represented by f , $f_{\max}$ represents the maximum adaptation of the current population, $f_{\min}$ represents the minimum adaptation of the current population, the average adaptation of the current population is represented by f_{avg} represents the average fitness of the current population. From the above formula, it can be seen that the mutation probability is not fixed, but can change at any time, the change is based on the degree of chromosome precocity and the fitness value of each individual to be mutated.

III. A. 4) Algorithmic flow

(1) In order to generate the initial population P, it needs to be encoded in real numbers.

(2) In order to derive the average value of population fitness (AVG), it is necessary to first define its fitness function and calculate the fitness value in each individual (population).

(3) The genetic strategy will be determined precisely, the population size (N) will be screened, and a series of genetic operations will be performed.

(4) Determine the new generation of population fitness mean value can reach the predetermined number of iterations, if not reached need to return to step 2, or modify the strategy and return, if the standard is reached that is the end of the process.

In order to determine the accuracy of the genetic algorithm, simulation experiments were carried out on the VC++.net platform, where the user is free to operate and change the values at will, and ultimately obtain a complete model of ceramic artwork.

III. B. Analysis of different 3D printing task scheduling process

III. B. 1) Traditional 3D Printing Task Scheduling

Traditional 3D printing task scheduling in addition to manual allocation, the most important is the first-come-first-served (FCFS) task scheduling method, using the receipt of a task to assign a task to the task allocation, but this method is only applicable to the task volume or the printer is less, for the scale of the cluster 3D printing manufacturing is very prone to scheduling chaos, scheduling program unreasonable situation, and scheduling efficiency is too low. scheduling program is not reasonable, and the scheduling efficiency is too low. Sometimes there may be similar to a small volume of tasks in the large volume printer processing, and large volume tasks can not be idle in the small volume printer processing, can only be scheduled after the small volume of tasks, both resulting in a waste of resources, but also prolonged the printing time, increasing the cost of printing. The same because the printing speed of the printer is generally higher printing costs, in the traditional way of 3D printing task allocation, the printing speed of the printer is often assigned to more printing tasks, which leads to although the overall printing time is shorter, but the overall printing costs are higher.

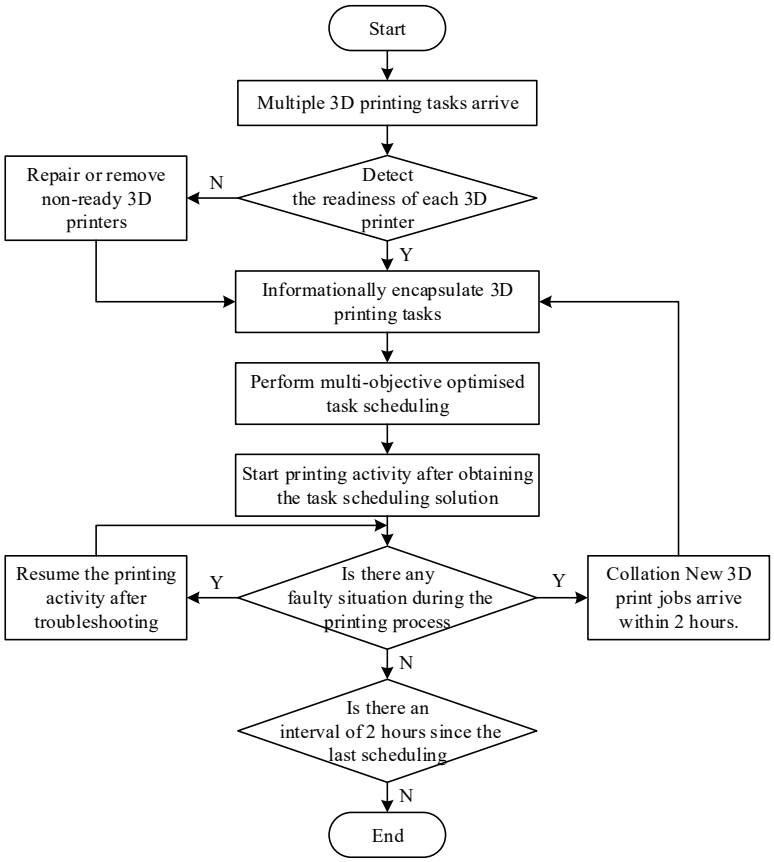

Figure 2: 3D printing multi-objective optimization task scheduling process

III. B. 2) 3D Printing Multi-Objective Optimization Task Scheduling

The first step is to identify how many 3D printers are available to perform the 3D printing task and information such as the printing method, printing material, printing cost, printing speed, printing accuracy, space size, etc. of these

3D printers. Secondly, determine the information of the 3D printing tasks that need to be printed such as the mode requirements, material requirements, model size, accuracy requirements, and task volume. Then based on the manufacturing enterprises are most concerned about the time and cost of the two indicators, according to the information obtained from the task scheduling related to the shortest printing time and the lowest cost of printing as the optimization objective to complete the task scheduling, task scheduling program, and finally according to the task scheduling program will be assigned to the corresponding printer to print the task.

Of course, in the actual printing and manufacturing process, the print job is dynamically arriving, the difficulty of reasonable matching between the print job and the printer will increase, in order to avoid the high load of the system due to the large amount of computation, and to make the task scheduling more accurate and efficient, the system will not immediately carry out a new round of task scheduling after the arrival of a new print job, but will carry out the task scheduling once after every 2 hours [28]. 3D Printing Multi-targeting The optimized task scheduling process is shown in Figure 2.

III. C. Modeling the Multi-objective Optimization Task Scheduling Problem for 3D Printing

III. C. 1) Definition of relevant issues

Let there be a total of M printers and N print jobs, the printing speed of the i th printer is v_i, the printing cost is p_i, and the job size of the j th print job is l_j, so the time $t_{(i,j)}$ for the i th printer to print the j th subtask is denoted as:

$$t_{(i,j)} = \frac{l_j}{v_i} \tag{4}$$

The print time matrix is represented as:

$$T = \begin{pmatrix} t_{(1,1)} & t_{(1,2)} & \cdots & t_{(1,N)} \\ t_{(2,1)} & t_{(2,2)} & \cdots & t_{(2,N)} \\ \vdots & \vdots & \ddots & \vdots \\ t_{(M,1)} & t_{(M,2)} & \cdots & t_{(M,N)} \end{pmatrix} \tag{5}$$

The cost $c_{(i,j)}$ for the i th printer to print the j th print job is denoted:

$$c_{(i,j)} = p_i \times l_j \tag{6}$$

The print cost matrix is expressed as:

$$C = \begin{pmatrix} c_{(1,1)} & c_{(1,2)} & \cdots & c_{(1,N)} \\ c_{(2,1)} & c_{(2,2)} & \cdots & c_{(2,N)} \\ \vdots & \vdots & \ddots & \vdots \\ c_{(M,1)} & c_{(M,2)} & \cdots & c_{(M,N)} \end{pmatrix} \tag{7}$$

The task scheduling scheme matrix X is denoted as:

$$X = \begin{pmatrix} x_{(1,1)} & x_{(1,2)} & \cdots & x_{(1,N)} \\ x_{(2,1)} & x_{(2,2)} & \cdots & x_{(2,N)} \\ \vdots & \vdots & \ddots & \vdots \\ x_{(M,1)} & x_{(M,2)} & \cdots & x_{(M,N)} \end{pmatrix} \tag{8}$$

where $x_{(i,j)}$ is a 0 - 1 decision variable, when $x_{(i,j)} = 1$ it means to print the j th print job on the i th printer, and when $x_{(i,j)} = 0$ it means that the j th print job is not printed on the i th printer.

In this paper, we refer to the first task scheduling of the system as primary scheduling and each subsequent scheduling as secondary scheduling. In the case of primary scheduling, the time for each printer to perform setup and the time for preheating and warming up is different, and in the case of secondary scheduling, the amount of tasks remaining on each printer from the previous job scheduling is different, which results in a different time for each printer to be able to start printing after the job scheduling is completed [29]. Calling the time from the start of

task scheduling to the time when the i th printer can print a new task as the initial time TS_i of that printer, the initial time matrix T_s can be expressed as:

$$T_s = \begin{pmatrix} TS_1 \\ TS_2 \\ \vdots \\ TS_M \end{pmatrix} \tag{9}$$

The time from the start of task scheduling until the j th print job is ready to print is referred to as the initial time tst_j of the j th print job, which can be denoted as:

$$tst_j = \begin{cases} \sum_{i=1}^{y} TS_i x_{(i,j)} + \sum_{i=1}^{y}\sum_{k=1}^{i-1} t_{(i,k)} x_{(i,k)} x_{(i,j)} & \sum_{i=1}^{y}\sum_{k=1}^{j} x_{(i,k)} x_{(i,j)} > 1 \\ \sum_{i=1}^{y} TS_i x_{(i,j)} & \sum_{i=1}^{y}\sum_{k=1}^{j} x_{(i,k)} x_{(i,j)} = 1 \end{cases} \tag{10}$$

The printing time tct_j of the j th print job is mainly divided into the initial time tst_j and the processing time $t_{(i,j)}$ of the j th print job on the i th printer, which can be expressed as follows:

$$tct_j = tst_j + t_{(i,j)} \tag{11}$$

III. C. 2) Constraints

Because of the one-shot nature of 3D printing, each print job can generally be assigned to only one printer, i.e:

$$\forall j \in [1, N], \sum_{i=1}^{M} x_{(i,j)} = 1 \tag{12}$$

Due to the limitations of print material, print mode, print accuracy, and space size, this print job can only print on this printer if the print job and the printer are perfectly matched, where the print material matching value of the j th print job and the i th printer is $dc_{(i,j)}$, the print mode matching value is $df_{(i,j)}$, the print accuracy matching value is $dj_{(i,j)}$, space size matching value is $ds_{(i,j)}$, and total matching value is $dz_{(i,j)}$, i.e:

$$\begin{aligned} &\forall i \in [1, M], j \in [1, N], dz_{(i,j)} \\ &= dc_{(i,j)} \times df_{(i,j)} \times dj_{(i,j)} \times ds_{(i,j)} = 1 \end{aligned} \tag{13}$$

III. C. 3) Objective function

The print time matrix T_1 for each printer to complete the print job assigned to that printer after completing one job schedule is denoted as:

$$\begin{aligned} T_1 &= XTE_M \\ &= \begin{pmatrix} x_{(1,1)} & x_{(1,2)} & \cdots & x_{(1,N)} \\ x_{(2,1)} & x_{(2,2)} & \cdots & x_{(2,N)} \\ \vdots & \vdots & \ddots & \vdots \\ x_{(M,1)} & x_{(M,2)} & \cdots & x_{(M,N)} \end{pmatrix}_s \begin{pmatrix} t_{(1,1)} & t_{(1,2)} & \cdots & t_{(1,N)} \\ t_{(2,1)} & t_{(2,2)} & \cdots & t_{(2,N)} \\ \vdots & \vdots & \ddots & \vdots \\ t_{(M,1)} & t_{(M,2)} & \cdots & t_{(M,N)} \end{pmatrix} \\ \begin{pmatrix} 1 & 0 & \cdots & 0 \\ 0 & 1 & \cdots & 0 \\ \vdots & \vdots & \ddots & \vdots \\ 0 & 0 & \cdots & 1 \end{pmatrix} &= \begin{pmatrix} \sum_j t_{(1,j)} x_{(1,j)} \\ \sum_j t_{(2,j)} x_{(2,j)} \\ \vdots \\ \sum_j t_{(M,j)} x_{(M,j)} \end{pmatrix} \end{aligned} \tag{14}$$

The completion time of a printer refers to the time from the start of job scheduling to the end of the last print job for that printer, including both the initial time and the print time, so the completion time matrix T_2 for each printer is denoted as:

$$T_2 = T_1 + T_s = \begin{pmatrix} \sum_j t_{(1,j)} x_{(1,j)} + TS_1 \\ \sum_j t_{(2,j)} x_{(2,j)} + TS_2 \\ \vdots \\ \sum_j t_{(M,j)} x_{(M,j)} + TS_M \end{pmatrix} \tag{15}$$

The total print time of a print job is the maximum of the completion times of all printers, so the total print time $f_T(X)$ to complete a print job is denoted:

$$f_T(X) = \max(T_2) = \max \begin{pmatrix} \sum_j t_{(1,j)} x_{(1,j)} + TS_1 \\ \sum_j t_{(2,j)} x_{(2,j)} + TS_2 \\ \vdots \\ \sum_j t_{(M,j)} x_{(M,j)} + TS_M \end{pmatrix} \tag{16}$$

One of the objectives of task scheduling is to minimize the total printing time, so the objective function f_T for time optimization can be expressed as:

$$f_T = \min(f_T(X)) = \min \left\{ \max \begin{pmatrix} \sum_j t_{(1,j)} x_{(1,j)} + TS_1 \\ \sum_j t_{(2,j)} x_{(2,j)} + TS_2 \\ \vdots \\ \sum_j t_{(M,j)} x_{(M,j)} + TS_M \end{pmatrix} \right\} \tag{17}$$

The total printing cost is the sum of the printing costs of all print jobs on the corresponding printers, so the total printing cost $f_C(X)$ can be expressed as:

$$\begin{aligned} f_C(X) &= \sum XC \\ &= \sum \left(\begin{pmatrix} x_{(1,1)} & x_{(1,2)} & \cdots & x_{(1,N)} \\ x_{(2,1)} & x_{(2,2)} & \cdots & x_{(2,N)} \\ \vdots & \vdots & \ddots & \vdots \\ x_{(M,1)} & x_{(M,2)} & \cdots & x_{(M,N)} \end{pmatrix}_s \begin{pmatrix} c_{(1,1)} & c_{(2,1)} & \cdots & c_{(M,1)} \\ c_{(1,2)} & c_{(2,2)} & \cdots & c_{(M,2)} \\ \vdots & \vdots & \ddots & \vdots \\ c_{(1,N)} & c_{(2,N)} & \cdots & c_{(M,N)} \end{pmatrix} \right) \\ &= \sum_i \sum_j c_{(i,j)} x_{(i,j)} \end{aligned} \tag{18}$$

One of the objectives of job scheduling is to minimize the total printing cost, so the objective function f_C for cost optimization can be expressed as:

$$f_C = \min(f_C(X)) = \min \left(\sum_i \sum_j c_{(i,j)} x_{(i,j)} \right) \tag{19}$$

In order to satisfy the two optimization objectives of time and cost at the same time when completing the printing task, the n-paradigm weighting method is used to assign the corresponding weights for the printing time optimization objective and the printing cost optimization objective, and a combined objective optimization model based on printing time and printing cost is designed, and its objective function H can be expressed as follows:

$$\begin{aligned} H &= \min\left(H(X)\right) \\ &= \min\left(\sqrt{\omega_1\left(\frac{f_C(X)-f_C}{f_C}\right)+\omega_2\left(\frac{f_T(X)-f_T}{f_T}\right)}\right) \end{aligned} \tag{20}$$

$$\omega_1+\omega_2=1 \tag{21}$$

where $H(X)$ is the combined evaluation metric value of printing time and printing cost, and the weights of printing time and printing cost are ω_1 and ω_2 respectively.

III. D. Problem solving based on improved particle swarm algorithm

III. D. 1) Particle Swarm Algorithm

Particle swarm optimization algorithm is a group intelligence optimization algorithm, through the simulation of bird foraging behavior, each bird as an independent foraging individual, through the transmission of information, so that the other birds know their own position and food, so as to determine whether the food they find is optimal or not, so as to find the global optimum by using the group of individuals in the information sharing and collaboration.

The particle swarm algorithm represents birds through a group of massless independent particles, each particle has only two parameters, position vector and velocity vector, which represent the position of the particle as well as the speed and direction of the movement. In the intelligent optimization process, each particle searches for the optimal solution individually and records it. According to the continuous updating of the fitness, i.e., the value of the objective function, the current individual optimal value P_{best} and the global optimal value G_{best} are recorded after the sharing of the position information and the value of the objective function among the swarm of particles. After the continuous iteration of the algorithm, the particle swarms move towards the optimal position, and finally arrive at the global optimal solution and position.

For the multi-machine-multi-task 3D printing scheduling problem, we try to make targeted improvements in the encoding method and update strategy. Firstly, a decimal sequential two-dimensional coding method is adopted to represent the solution of the problem, and a dynamic ω with linearly decreasing weights is applied to the updating strategy to adjust the global and local search ability.

III. D. 2) Encoding and decoding schemes

The complexity of the 3D printing scheduling problem for multi-machine multi-tasking is such that not only the combined scheduling of parts needs to be taken into account in the coding process, but also the selection of an appropriate processing machine for all the parts in a job is required, and thus it is not achievable to use only a one-dimensional coding of the parts. Therefore, a decimal sequential two-dimensional encoding is used to represent the solution of the problem [30]. The first part is a machine-based encoding for determining the choice of machining machine for each part, and the second part is a sequential part-based encoding for determining the order in which the parts are combined for machining. With this two-dimensional coding approach, a feasible solution to the problem can be obtained.

III. D. 3) Population initialization

Generally, as the number of iterations increases, the search time of the algorithm increases, but the results of the search may be better, so for the particle swarm algorithm, it is important to choose the appropriate number of iterations with the number of populations. Generally, the population number is taken from 20 to 50, and the exact value depends on the complexity of the research problem. For the multi-machine multi-task 3D printing scheduling problem, the population number P_N is set to 50 and the number of iterations I_N is set to 300 because it is more complex.

The initial positions of the particles are uniformly distributed throughout the search space, and the initialization process initializes the particle swarm as a group of random particles that can represent the solution of the problem, and each particle contains machine vectors and order vectors two-dimensional real numbers, and the value space of the vector values is $[1,m]$, and m is the total number of machines. The initial speed can be set to 0 or a random value. The corresponding initial fitness function, i.e., the cost per unit volume value, is taken as the individual optimal solution.

In the initial setting of the speed, when set to 0, the particles and the search space are static, when the speed is non-zero, taking into account that when the particle speed is larger, the particles move faster and are easy to miss the optimal solution, thus increasing the number of iterations and improving the complexity of the algorithm, when it is smaller, the development ability is strong, but it is easy to fall into the local optimum, convergence is slow, and the algorithm is not very efficient. Therefore, in order to reasonably seek the balance between the algorithm search ability and convergence speed, the maximum speed of the particles is set, which is usually set as the range width of the particles, and keep the variable change in the range of 10% to 20%.

III. D. 4) Update strategy

After initialization as a group of random particles, these particles get the optimal solution by continuously sharing the position and optimal value between the individuals and the group, and updating the position and objective function value after iteration. In each iteration of the algorithm, the optimal value P_{best} of the current individual as well as the global optimal solution G_{best} are recorded, after which one updates one's velocity and position.

The diversity of the population, i.e., the differences on the individual particles, determines the global exploration ability of the algorithm, so it is important to keep the differences among the particles when updating the individual particles to learn to move towards the optimal solution. In the early stage of the particle swarm algorithm search, it is often hoped that more fields can be searched quickly and the approximate range of the global optimum can be determined, while in the later stage of the search, it is often hoped that the local optimal solution can be found quickly and accurately to complete the convergence, so in the whole iterative process of the algorithm, the search requirements and hopes are not unchanging.

When the individual particles are approaching the optimal solution, they adjust their own trajectory to a certain extent and carry out the exploration of the unknown field, and this exploration ability is the global exploration ability. The further exploration on the original trajectory is called local exploration ability. In order to effectively prevent from falling into local optimization, the dynamic ω with linearly decreasing weights is used to adjust the global and local search ability. The ω is also known as the inertia factor and takes a non-negative value. When ω takes a larger value, the global search ability is stronger, while the local search ability is weaker. When ω is small, the global search ability is weak, while the local search ability is strong. In general, in practical applications, the value of ω is changed from large to small, the first global optimal search to the approximate range, and then search for the optimal value in the local search to improve efficiency and accuracy.

Inertia factor ω update formula is as follows:

$$\omega_t = (\omega_{ini} - \omega_{end})(G_k - g) / G_k + \omega_{end} \tag{22}$$

where: G_k is the maximum number of iterations, ω_{ini} is the initial inertia weights, and ω_{end} is the inertia weights at the time of iteration to the maximum number of iterations, which is generally taken as $\omega_{ini} = 0.9$ and $\omega_{end} = 0.4$, thus favoring the convergence of the algorithm at a later stage.

The velocity update formula is as follows:

$$v_{i+1} = \omega \times v_i + c_1 \times rand(\ ) \times \left(P_{best_i} - x_i\right) + c_2 \times rand(\ ) \times \left(G_{best} - x_i\right) \tag{23}$$

where: v_{i+1} is the velocity of the particle, $rand(\ )$ represents a random value between (0, 1), c_1, c_2 are the learning factors, usually $c_1 = c_2 = 2$, and x_i is the current position of the particle.

The PSO algorithm does not have the cross mutation operation like the genetic algorithm, but simply updates the search to follow the optimal particle based on its own experience. Eq. (8) contains the sum of three parts, the first part represents the effect of the last velocity vector, the second part is called the self-cognition term, which represents the vector based on the individual experience particles to move toward their own optimal solution, and the third part is called the group-cognition term, which represents the vector based on the experience particles of the individual and the group to move toward the global optimal solution.

The position update formula is as follows:

$$x_{i+1} = x_i + v_{i+1} \tag{24}$$

The population updates the velocity and position vectors during the iteration process according to Eq.

III. D. 5) Basis for convergence

Optimization convergence stopping criterion generally has two kinds, one is to set the maximum number of iterations, and the other is to reach the acceptable satisfactory fitness value, set the difference between the last optimal fitness

value and the updated optimal fitness value is less than a certain value to stop the iteration, that is, to reach the convergence requirements. In this study, the convergence criterion is set as whether the number of iterations to reach 300 times, after reaching the convergence criterion, it will exit the loop and output the results.

III. D. 6) Algorithmic flow

For the multi-machine multi-task 3D printing scheduling problem, based on the improved particle swarm algorithm, the objective function is set to the average cost per unit volume, considering the bottom area of the machine table and the maximum height of the support and other constraints, and ultimately obtaining the optimal value of the cost per unit volume and the optimal scheduling scheme through continuous iterative optimization.

The flow of the improved particle swarm algorithm is shown in Figure 3.

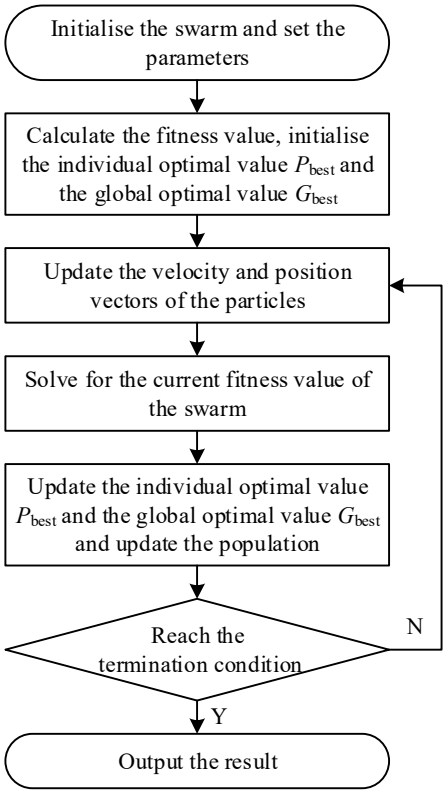

Figure 3: Improved particle swarm algorithm process

IV. Experimental results and analysis

IV. A. Genetic Algorithm Performance Test

In order to verify the effectiveness of the algorithm, the standard function is selected for testing in this section, and the test results are shown in Fig. 4. The simulation graph can be seen that the genetic algorithm proposed in this paper yields results that match well with the Pareto frontier, which also proves the effectiveness of the algorithm in this paper to some extent.

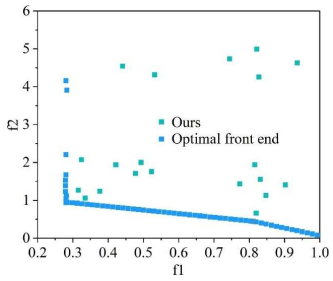

Figure 4: Test results

IV. B. Example validation

In order to test the optimization effect of the established multi-objective optimization model, the ceramic artwork model is selected as the optimization object, and some control parameters in the algorithm are set as follows: the population size is 100, the crossover probability is 0.9, the variance probability is 0.1, and the range of the delamination thickness is initially selected to be 0.089~0.203mm. The maximum number of generations of the program is 80 and 100 generations, respectively, The optimization of the molding direction and delamination thickness for the maximum evolutionary generations of 80, 100 and 150, respectively, and the Pareto front under the same evolutionary generations is shown in Fig. 5. From the figure, it is easy to find that, when the algorithm controls the parameter population size, the probability of cross-variation is unchanged, the evolutionary generations of 80, 100 and 150 generations, respectively, to obtain different evolutionary generations under the Pareto front performance is quite stable, and it can be considered that the overall trend is the same, but only the sparsity of the points on the Pareto front is slightly different. Therefore, it can be assumed that the use of 100 generations is sufficient to find a solution that meets the requirements.

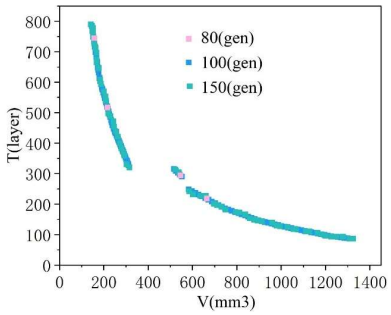

Figure 5: Pareto front edge of different evolutionary algebra

In the case of 100 generations of evolution and other control parameters are the same as above, we observe the evolution process from the 1st generation until the last generation and analyze the ability of the algorithm in global optimization search. The population change in the case of 100 generations of evolution is shown in Fig. 6. From the figure, it can be seen that the population keeps approaching towards the final Pareto frontier as the population generations are updated. In generation 1, the algorithm uses random selection method to obtain individuals in the feasible domain to form the initial population, which leads to uneven individuals in the population space, and the corresponding objective function values are also distributed in a messy way, requiring further optimization and selection. By the 10th generation, the individuals of the population have initially formed the shape of Pareto frontier, i.e., the population retains the better individuals and excludes the poorer individuals through competition and elite strategy, indicating that the population space gradually moves towards the Pareto frontier through evolution. In the 50th generation, the individuals in the population space have approached the final Pareto front and even overlapped with it, indicating that the individuals in the population are basically all excellent individuals, i.e., they are all solutions that satisfy the requirements. Continuing the evolution until the 100th generation, the individuals in the population no longer continue to move but remain on the Pareto front, only that the individuals show a constant clustering on the Pareto front.

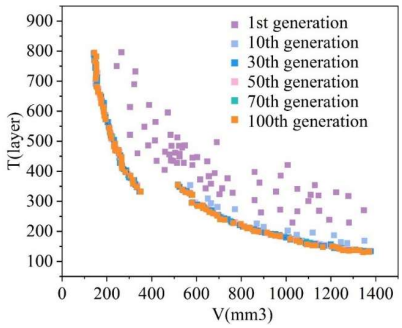

Figure 6: In the case of evolutionary algebra for 100 generations

In order to verify that the model can solve the problem of trade-off selection between molding quality and molding efficiency in 3D printing, and realize the purpose of intelligent selection of molding direction and layering thickness.

The Pareto frontier when the evolutionary generation is 100 generations is shown in Figure 7, in which ΔV, T represents the molding quality, molding efficiency, respectively, there is indeed a contradictory relationship, i.e., when the requirement of better molding quality, it will inevitably lead to an increase in the number of molding layers, which in turn will reduce the molding efficiency. When higher molding efficiency is required, it will inevitably lead to a decrease in molding quality. Thus, to satisfy the optimum molding quality, the volume error ΔV must be minimized, i.e., point A (145.32, 785) in the figure. At this point, the values of each design variable corresponding to this point are shown in Table 1. Therefore, the molding direction that makes the molding quality optimal should be along the -Z direction in the figure, with a delamination thickness of 0.085 mm. Similarly, to satisfy the highest molding efficiency, it is necessary to minimize the molding time T, i.e., point B (1326.35, 122) in the figure. Therefore, the molding direction that makes the molding efficiency optimal should be along the -Y direction in the figure, and the delamination thickness is 0.201 mm. Although points A and B in the figure make the molding quality optimal and the molding efficiency highest, respectively, but whether it is point A or B, the other objective corresponding to it is the worst among all the other points. In the case of single-objective optimization, the solutions corresponding to points A and B are the optimal solutions with the best molding quality and the highest molding efficiency, respectively. According to the definition of minimum distance, the point closest to the ideal point is found as the optimal solution, i.e., θ_1 =180°,h=0.201mm, ΔV =336.22mm3,T=342.

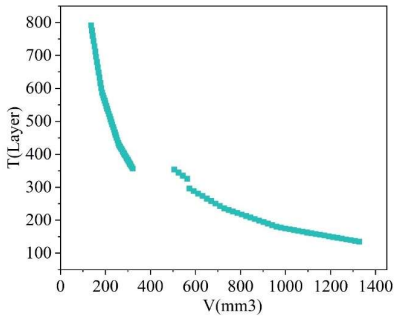

Figure 7: Evolutionary algebra is the front edge of the pareto

Table 1: Optimized result

	θ_1	θ_2	h(mm)	ΔV (mm^3)	T(layer)	Model height(mm)
Best molding	180°	~	0.085	145.32	785	76
Highest molding efficiency	90°	270°	0.201	1326.35	122	25.1
Final optimization solution	180°	~	0.201	336.22	342	76

In order to understand the relationship between the effect of layering thickness on forming quality and forming efficiency, among the 100 Pareto solutions obtained, all the solutions in the forming direction -Z direction that make the forming quality optimal are analyzed, and the relationship between forming quality, forming efficiency and layering thickness is plotted. The relationship between molding quality, molding efficiency and layering thickness in the Z-direction is shown in Fig. 8, where the volumetric error ΔV increases with the increase of layering thickness under the condition of constant molding direction, the molding quality of the ceramic artwork decreases, while its molding efficiency is improved. On the contrary, as the thickness of layering decreases, the volume error ΔV decreases, the molding quality of the ceramic artwork improves, and its molding efficiency decreases. This is because in a certain molding direction, the smaller the thickness of the delamination, the less pronounced the step effect produced by the delamination, the smaller the volume error caused by the step effect, the better the quality of the molded part. The smaller the thickness of the delamination, the more the number of layers obtained by delamination, the longer the time used for molding parts, the lower the molding efficiency. In view of this contradiction, when choosing the layering thickness of the part, it is also necessary to take into account the two factors of molding quality and molding efficiency, and comprehensively meet the requirements of molding quality and molding efficiency, in order to obtain satisfactory parts.

IV. C. Analysis of the results of the perceptual imagery evaluation

Perceptual imagery is the sensual impressions and representations of things formed by people in the process of perception and thinking, and is the connection between subjective feelings and objective things. Through analyzing and exploring perceptual imagery, we can deeply understand users' needs and feelings, and improve the

satisfaction and user experience of product design. This section mainly focuses on the research and analysis of the style of 18 pieces of ceramic artworks based on 3D printing technology by the method of perceptual imagery.

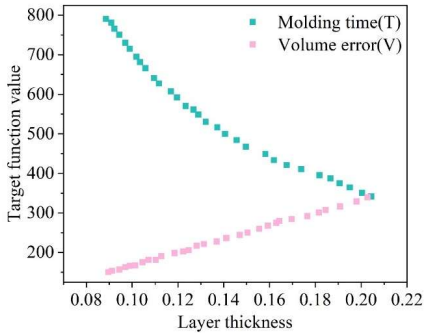

Figure 8: The relationship between forming quality, forming efficiency and stratification thickness

IV. C. 1) Factor analysis

The questionnaire data were imported into SPSS for factor analysis, 10 pairs of perceptual vocabulary were set as variables, factors with eigenvalues greater than 1 were extracted using the principal component extraction method, and the maximum variance method was used for factor rotation, and the results of the factor analysis are as follows:

(1) Reliability and validity analysis

The results of the reliability analysis of the perceptual vocabulary questionnaire are shown in Table 2. As can be seen from the table, the standardized Clonbach's α coefficient of the perceptual vocabulary questionnaire based on the style of ceramic artwork with 3D printing technology is 0.832, which indicates that there is excellent internal consistency within the scale, and therefore the credibility of the research results is very high, and it can be subjected to the next step of validity analysis.

Table 2: Analysis of the analysis of emotional vocabulary questionnaire

Clonbach	Clonbach based on standardization	Term number
0.779	0.832	10

Validity analysis refers to the coincidence of the measurement results with the real situation and determines whether the research data can be analyzed in the next step of factor analysis, generally using Bartlett's test and KMO test. The KMO and Bartlett values of the perceptual vocabulary questionnaire are shown in Table 3. From the table, the KMO value is 0.722, while the significance Sig value is less than 0.05, which is suitable for factor analysis.

Table 3: The emotional vocabulary questionnaire KMO and bartlett values

KMO sampling availability number		0.722
Bartlett sphericity test	Approximate card	192.35
	Freedom	46
	Significance	0

(2) Number of factors extracted

The factors were extracted through SPSS using principal component analysis and the total variance explained is shown in Table 4. As can be seen from the table, the eigenvalue of the first common factor solution is 5.723, which explains 57.24% of the total variance information of all variables, and it is a principal component that contributes the most variance. The eigenvalue of the second common factor solution is 2.457 and it explains 24.57% of the total variation information of all variables. The first two factor solutions explain a total of 81.81% of the total variance information of all variables, and from the third factor solution onwards, the eigenvalues are all less than 1. Therefore, the first 2 factor solutions can be extracted as common factors.

Table 4: The total variance of the explanation

Constituent	Initial eigenvalue			Extracting the load of the load			Rotational load squared		
	Total	Variance%	Cumulation%	Total	Variance%	Cumulation%	Total	Variance%	Cumulation%
1	5.723	57.24	57.24	5.723	57.24	57.24	5.139	52.921	52.921
2	2.457	24.57	81.81	2.457	24.57	81.81	3.041	28.291	81.212
3	0.89	8.90	90.71						
4	0.364	3.64	94.35						
5	0.201	2.01	96.36						
6	0.147	1.47	97.83						
7	0.128	1.28	99.11						
8	0.045	0.45	99.56						
9	0.026	0.26	99.82						
10	0.017	0.17	100						

The variation of principal component eigenvalues gravel plot is shown in Fig. 9, as can be seen from the figure, from the third factor solution the curve starts to regionally flatten out, so that 2 male factors can be extracted.

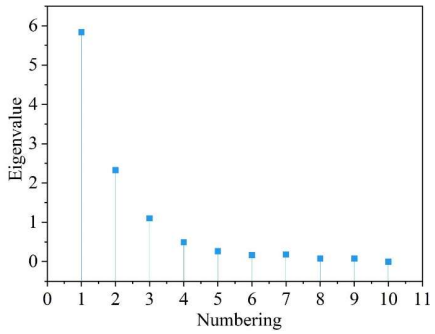

Figure 9: The change of the main component eigenvalue

(3) Factor extraction naming

The unrotated factor loading matrix is shown in Table 5, and the factor loading matrix after the rotation is shown in Table 6, according to the further differentiation of the rotated component matrix loading size, the relationship between the variables and the factors is clearer, so through the table rotated factor loading matrix can be extracted 2 male factors, the first factor of the variables have high-end-cheap, smart -deadly, futuristic-traditional, textured-non-textured, refined-rough, dexterous-bulky, named as style factor. The variables of the second factor are fantastic-plain, practical-decorative, simple-complex, rounded-mechanical, named as structure factor.

Table 5: Unrotated factor load matrix

	constituent	
	1	2
Round - mechanical	0.695	-0.312
Simple - complex	-0.257	0.918
High-end - cheap	0.872	0.374
Dreamy - plain	0.87	-0.398
Future - traditional	0.936	0.155
Daft - bulky	0.577	0.371
Delicate - rough	0.972	-0.041
Smart - rigid	0.933	0.259
Practical - decorative	-0.479	0.799
Textured-untextured	0.755	0.382

Table 6: Then the factor load matrix

	constituent	
	1	2
Round - mechanical	0.491	0.595
Simple - complex	0.185	-0.936
High-end - cheap	0.955	0.066
Dreamy - plain	0.596	0.746
Future - traditional	0.901	0.286
Daft - bulky	0.668	-0.076
Delicate - rough	0.852	0.479
Smart - rigid	0.935	0.199
Practical - decorative	-0.072	-0.936
Textured-untextured	0.851	0.002

IV. C. 2) Imagery Scale Maps

Imagery is the process of forming imagination, conjecture, imagination, association and other thinking activities in people's thinking activities. Through the image scale method, the corresponding product can be described more completely with as few image dimensions as possible through statistical dimensionality reduction, and at the same time, it can reflect the overall image tendency of the product. Multiply the eigenvectors with the normalized data to obtain the principal component data for each sample, as shown in Table 7. Through the analysis, it is found that the two groups of adjective factors of "concise-complex" and "futuristic-traditional" can be used to summarize the image-scale distribution characteristics of the whole sample. "Concise" is manifested in the fact that the ceramic artwork has few decorative structures, strong integration, and no complex and diverse colors. "Complex" is manifested as having more structures and a stronger sense of visual impact. The "futuristic" is more modern. The "traditional" performance is that the shape of the product retains many elements of the design and creation of traditional ceramic artworks.

Table 7: Main component data

Sample number	Main component 1	Main component 2	Sample number	Main component 1	Main component 2
Sample 1	-3.065	1.432	Sample 10	-0.022	1.221
Sample 2	1.446	1.944	Sample 11	3.341	-0.652
Sample 3	4.952	1.153	Sample 12	2.293	-0.332
Sample 4	0.592	0.436	Sample 13	2.611	0.811
Sample 5	0.012	-3.402	Sample 14	0.233	-0.231
Sample 6	1.547	-1.133	Sample 15	-3.876	1.269
Sample 7	-1.559	-3.755	Sample 16	-2.963	0.346
Sample 8	-2.336	0.305	Sample 17	0.356	0.172
Sample 9	-1.265	-0.159	Sample 18	-2.206	0.466

IV. C. 3) Analysis of ceramic artwork modeling based on sensual imagery

In order to better analyze the relationship between different types of products and their corresponding influence factors, it can be analyzed on the basis of the sample evaluation line graph combined with the previously extracted common factor, combined with the sample evaluation after the extraction of the common factor is shown in Figure 10. Among the influence variables of the style factor are high-end - cheap, smart - rigid, futuristic - traditional, textured - untextured, delicate - rough, dexterous - bulky. Influence variables of structural factors are fantastic-plain, practical-decorative, simple-complex, rounded-mechanical. According to the figure, it can be found that among the 6 influencing variables of the style factor, Sample 3 and Sample 13 correspond to perceptual vocabularies that are more high-end, futuristic, and sophisticated. Among the 4 influencing variables of the structure factor, the perceptual vocabulary corresponding to Sample 2 and Sample 3 is more inclined to mellow, simple, and practical.

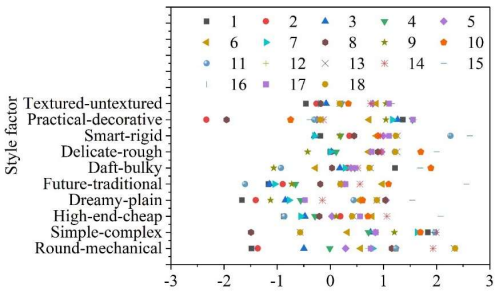

Figure 10: The sample evaluation of the extraction of the male factor

V. Conclusion

With the continuous development of science and technology, 3D printing technology has been widely used in many fields. This paper aims to discuss the application of 3D printing technology in the creation of ceramic artwork.

Through the example analysis, over the optimization of the personalized ceramic artwork, it is known that the procedure is feasible, and the combination of the optimal molding direction and layering thickness of the personalized ceramic artwork model is obtained as θ_1 =180°,h=0.201mm, ΔV =336.22mm3,T=342.

In the experiment of analyzing the styling of ceramic artwork based on perceptual imagery, among the six influencing variables of the style factor, the perceptual vocabulary corresponding to Sample 3 and Sample 13 is more skewed towards high-end, futuristic, and exquisite. It can be concluded that the ceramic artwork designed based on the method of this paper is more personalized and diversified in terms of styling.

In summary, 3D printing technology has an important role, value and development prospects in the creation of personalized ceramic art. We need to continue to pay attention to technology research and development, and actively explore new application modes, 3D printing technology brings infinite possibilities and opportunities for ceramic art creation, and contributes wisdom and strength to the prosperity and development of ceramic art.

References

[1] Zhang, R. Z., & Reece, M. J. (2019). Review of high entropy ceramics: design, synthesis, structure and properties. Journal of Materials Chemistry A, 7(39), 22148-22162.

[2] Huang, Q., Lin, H., Wang, B., Lin, S., Wang, P., Sui, P., ... & Wang, Y. (2022). Patterned glass ceramic design for high-brightness high-color-quality laser-driven lightings. Journal of Advanced Ceramics, 11(6), 862-873.

[3] Pampuch, R., & Pampuch, R. (2014). A brief history of ceramic innovation. An Introduction to Ceramics, 1-17.

[4] Yueming, H. (2021). Research on the role of art creation in ceramic material product design based on the perspective of innovation. In E3S Web of Conferences (Vol. 251, p. 01033). EDP Sciences.

[5] Xie, Q., & Lei, Z. (2024). Research on the Innovation of Ceramic Art Products Based on CAD Technology Optimization. Computer-Aided Design and Applications, 218-231.

[6] He, Y. (2022). Research on innovative thinking of ceramic art design based on artificial intelligence. Mobile Information Systems, 2022(1), 3381042.

[7] Khosravani, M. R., & Reinicke, T. (2020). On the environmental impacts of 3D printing technology. Applied Materials Today, 20, 100689.

[8] Karakurt, I., & Lin, L. (2020). 3D printing technologies: techniques, materials, and post-processing. Current Opinion in Chemical Engineering, 28, 134-143.

[9] Chen, Z., Li, Z., Li, J., Liu, C., Lao, C., Fu, Y., ... & He, Y. (2019). 3D printing of ceramics: A review. Journal of the European Ceramic Society, 39(4), 661-687.

[10] Hwa, L. C., Rajoo, S., Noor, A. M., Ahmad, N., & Uday, M. B. (2017). Recent advances in 3D printing of porous ceramics: A review. Current Opinion in Solid State and Materials Science, 21(6), 323-347.

[11] Kamran, M., & Saxena, A. (2016). A comprehensive study on 3D printing technology. MIT Int J Mech Eng, 6(2), 63-69.

[12] Manero, A., Smith, P., Sparkman, J., Dombrowski, M., Courbin, D., Kester, A., ... & Chi, A. (2019). Implementation of 3D printing technology in the field of prosthetics: Past, present, and future. International journal of environmental research and public health, 16(9), 1641.

[13] Rayna, T., & Striukova, L. (2021). Assessing the effect of 3D printing technologies on entrepreneurship. Technological Forecasting and Social Change, 164, 120483.

[14] Diao, Q., Zeng, Y., & Chen, J. (2024). The applications and latest progress of ceramic 3D printing. Additive Manufacturing Frontiers, 3(1), 200113.

[15] Hu, L. (2020). Application of AutoCAD's 3D modeling function in industrial modeling design. Computer-Aided Design and Applications, 18(1).

[16] Huang, T. C., & Lin, C. Y. (2017). From 3D modeling to 3D printing: Development of a differentiated spatial ability teaching model. Telematics and Informatics, 34(2), 604-613.

[17] Beknazarova, S. S. (2016). 3D modeling and the role of 3D modeling in our life. In International scientific and practical conference world science (Vol. 3, No. 3, pp. 28-31). ROST.

[18] Liu, B., Wu, Y., Xing, W., Guo, S., & Zhu, L. (2023). The role of self-directed learning in studying 3D design and modeling. Interactive Learning Environments, 31(3), 1651-1664.

[19] Abdelkader, M., Petrik, S., Nestler, D., & Fijalkowski, M. (2024). Ceramics 3D printing: a comprehensive overview and applications, with brief insights into industry and market. Ceramics, 7(1), 68-85.

[20] Owen, D., Hickey, J., Cusson, A., Ayeni, O. I., Rhoades, J., Deng, Y., ... & Zhang, J. (2018). 3D printing of ceramic components using a customized 3D ceramic printer. Progress in additive manufacturing, 3, 3-9.
[21] Wang, Y., Wu, T., & Huang, G. (2024). State-of-the-art research progress and challenge of the printing techniques, potential applications for advanced ceramic materials 3D printing. Materials Today Communications, 110001.
[22] Choi, J. H., & Kim, W. S. (2019). A case study of ceramic design that combines 3D printing technology. Journal of digital convergence, 17(4), 309-317.
[23] Mei, H., Tan, Y., Huang, W., Chang, P., Fan, Y., & Cheng, L. (2021). Structure design influencing the mechanical performance of 3D printing porous ceramics. Ceramics International, 47(6), 8389-8397.
[24] Faes, M., Valkenaers, H., Vogeler, F., Vleugels, J., & Ferraris, E. (2015). Extrusion-based 3D printing of ceramic components. Procedia Cirp, 28, 76-81.
[25] Bose, S., Akdogan, E. K., Balla, V. K., Ciliveri, S., Colombo, P., Franchin, G., ... & Bandyopadhyay, A. (2024). 3D printing of ceramics: Advantages, challenges, applications, and perspectives. Journal of the American Ceramic Society, 107(12), 7879-7920.
[26] Zhang, F., Li, Z., Xu, M., Wang, S., Li, N., & Yang, J. (2022). A review of 3D printed porous ceramics. Journal of the European Ceramic Society, 42(8), 3351-3373.
[27] Xinyu Feng,Xijing Zhu,Wei Zhao & Chao Yan. (2024). Coupling mechanical model and failure of aeroengine ceramic matrix composite based on genetic algorithm. Measurement: Sensors,33,101226-.
[28] Liu Sicheng,Zhang Lin,Zhang Weiling & Shen Weiming. (2021). Game theory based multi-task scheduling of decentralized 3D printing services in cloud manufacturing. Neurocomputing,446,74-85.
[29] Longfei Zhou,Lin Zhang,Yuanjun Laili,Chun Zhao & Yingying Xiao. (2018). Multi-task scheduling of distributed 3D printing services in cloud manufacturing. The International Journal of Advanced Manufacturing Technology,96(9-12),3003-3017.
[30] Husam Kaid,Abdulmajeed Dabwan,Khaled N. Alqahtani,Emad Hashiem Abualsauod,Saqib Anwar,Ali M. Al Samhan & Abdullah Yahia AlFaify. (2023). Optimization of the Effect of Laser Power Bed Fusion 3D Printing during the Milling Process Using Hybrid Artificial Neural Networks with Particle Swarm Optimization and Genetic Algorithms.Processes,11(10).